Supplemental Figure Legends:

Supplemental Figure 1. FANCJ is recruited to sites of UV-induced damage in an NER dependent manner (A) *XP-F* cells expressing vector, XPF^{WT}, or XPF^{D676A} were globally UV irradiated (5 J/m^2). At 3h after UV irradiation, cells were processed and co-immunostained with the indicated Abs. (B) Quantification of cells with FANCJ-positive foci. (C) A549 cells containing unique shRNA vectors targeting FANCJ or NSC were UV irradiated through micropore filters, co-immunostained with the indicated Abs at several time points and quantified for cells with ERCC1 positive LUDS and (D) XPC positive LUDs. Where shown, error bars represent the standard deviation of the mean of three independent experiments

Supplemental Figure 2. MMR localizes FANCJ to UV induced LUDs (A) U2OS cells containing a second shRNA vector targeting MSH2 or NSC were analyzed by immunoblot and (B) UV irradiated through micropore filters and quantified for cells with FANCJ- or 6-4 PP-positive LUDs. (C) U2OS cells containing two distinct shRNA vectors targeting MSH6 or NSC were analyzed by immunoblot and (D) treated as in B and quantified for cells with FANCJ- or 6-4 PP-positive LUDs. (E) U2OS cells containing shRNA vectors targeting MSH2 or NSC were UV irradiated through micropore filters and co-stained with XPC and ERCC1 abs. Representative images are shown 2 h after UV irradiation. (F) Quantification of cells with XPC- or ERCC1-positive LUDs. (G) *XP-F* cells complemented with empty vector or XPF^{WT} were UV irradiated through micropore filters and co-stained with MSH2 and ERCC1 abs. Representative images are shown 2 h after UV irradiation. (H) Quantification of *XP-F* cells with MSH2- or ERCC1-positive LUDs. (I) *XP-F* cells containing shRNA vectors targeting MSH2 or NSC were UV irradiated through micropore filters, pre-extracted with 0.5% Triton-X in PBS prior to fixation, and co-immunostained with the indicated Abs, a representative image is shown 2 hrs post UV irradiation. Where shown, error bars represent the standard deviation of the mean of three independent experiments

Supplemental Figure 3. FANCJ localizes to UV induced LUDs predominantly in S-Phase and contributes to the UV induced checkpoint (A) 48BR cells were UV irradiated through micropore filters prior to incubation with 10uM EdU for 3 hrs. Cells were then processed for EdU incorporation and co-immunostained with the indicated Abs. (B) Quantification of co-localization of XPF, FANCJ, MLH1, or MSH2 with LUDs in non-S phase cells representing sites of gap filling and (C) quantification of co-localization of XPF, FANCJ, MLH1, or MSH2 with LUDs in S-phase cells. (D) Whole cell extracts of MCF7 cells containing shRNA vectors targeting FANCJ or NSC were analyzed by immunoblot with the indicated Abs at the indicated time points after UV irradiation. The ratio of phospho-protein/total protein by densitometry using Image J software is quantified.

Supplemental Figure 4. FANCJ and MMR function in a common pathway for RPA phosphorylation and 6-4 Photoproduct elimination, but not for gap repair. (A) A549 cells containing shRNA vectors targeting FANCJ or NSC were stably depleted of MSH2 versus a second NSC and analyzed for immunoblot or (B) UV irradiated through 5 um filters to generate LUDs and co-immunostained with the indicated Abs at several time points and quantified for cells with phospho-serine4/8 RPA32-positive LUDs and (C) 6-4 PP-positive LUDs. (D) 48BR cells containing shRNA vectors targeting XPF, FANCJ-1, FANCJ-2, MLH1, MSH2 or NSC were UV irradiated through micropore filters prior to incubation with 10uM EdU for 3 hrs and quantified for gap-filling in non-S cells. (E) MSH2 isogenic mouse embryonic fibroblasts were analyzed by immunoblot, treated as in A,

and quantified for gap filling in non- S phase cells. Where shown, error bars represent the standard deviation of the mean of three independent experiments.

Supplemental Figure 5. FANCJ precipitates with UV modified PCNA and CPD from chromatin extracts. (A) A549 cells were left untreated or globally UV irradiated and collected in 150 nM NETN buffer. Cells were then spun down and the insoluble pellet was re-suspended in RIPA buffer and sonicated. The RIPA fraction was spun down and the chromatin lysate was used for input or for CPD immuno-precipitation (IP). IPs were then analyzed by immunoblot with the indicated Abs.

Supplemental Figure 6. FANCJ deficient cells are sensitive to DNA interstrand crosslinking agents and FANCJ suppresses UV-induced mutations (A) A549 cells expressing shRNA vectors targeting FANCJ or NSC were left untreated or treated with Cisplatin (CPPD) and analyzed for colony survival. (B) Quantification of surviving colonies. (C) *FA-J* cells expressing empty vector control or $FANCJ^{WT}$ were UV irradiated and analyzed for survival in 6-TG relative to untreated cells (D) Empty vector control- or $FANCJ^{WT}$-complemented *FA-J* cells were analyzed for relative survival after mitomycin C treatment. Cells were stained with crystal violet, solubilized, and absorbance was measured at 590nm. The relative absorbance of treated/untreated was quantified as relative survival. (E) *FA-J* cells were treated as in D, except analyzed for relative survival after UV irradiation. Where shown, error bars represent the standard deviation of the mean of three independent experiments.

Supplemental Figure 7. Mutations in FANCJ and MMR loci occur in melanoma genomes (A) FANCJ protein coding mutations were identified from sequenced melanoma genomes in cBioPortal and the Catalogue of Somatic Mutations in Cancer (CoSMiC) databases. Mutations are located throughout the FANCJ sequence as indicated. Two specific amino acids were previously identified, in hereditary breast cancer (blue) and in Fanconi Anemia (green). Mutations found in the iron-sulfur domain (red). Sites where FANCJ interacts with MLH1 (K141/K142) and BRCA1 (S990) are indicated. (B) FANCJ protein coding mutations (C) protein coding mutations identified in MSH2 as in A, (D) MSH6, (E) MLH1, and (F) PMS2.

Supplemental Figure 8. Ectopic expression of catalytic inactive $FANCJ^{K52R}$ disrupts clearance of UV induced lesions in U2OS cells (A) U2OS cells were transfected with pCDNA3 constructs containing vector, $FANCJ^{WT}$, or $FANCJ^{K52R}$ and analyzed by immunoblot wit the indicated Abs. (B) Cells were UV irradiated through 5 um filters to generate LUDs and co-immunostained with the indicated Abs 16h post treatment and (C) quantified for cells with phospho-serine4/8 RPA32-positive LUDs and 6-4 PP-positive LUDs.

Supplemental Figure 9. FANCJ expression promotes UV induced GFP-polh foci formation in U2OS cells (A) U2OS cells were transfected with GFP-polh and left untreated or globally UV irradiated and analyzed on a fluorescent microscope. (B) Cells were co-transfected with GFP-polh and siRNA reagents targeting luciferase control, FANCJ, or RAD18 and analyzed by immunoblot with the indicated Abs. (C) Cells were left untreated or globally UV irradiated quantified for cells with >5 GFP-polh foci.

Supplemental Table 1. FANCJ suppresses UV-induced mutations at the *HPRT* locus. Classification of clones with *HPRT*-inactivating mutations from A549 cells expressing shRNAs to FANCJ (combined) vs. NSC.

Supplemental 1

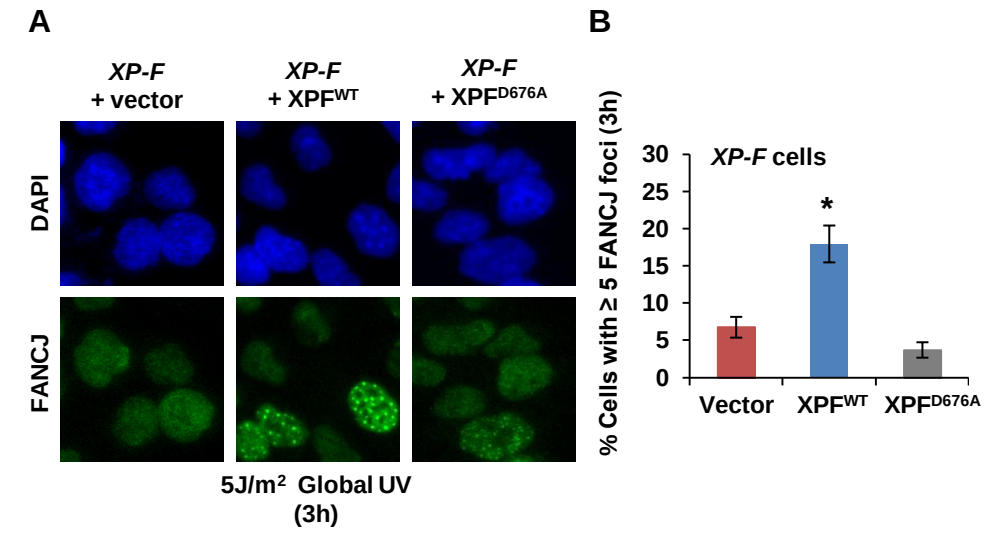

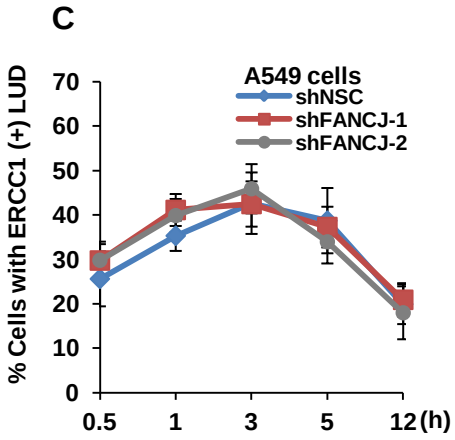

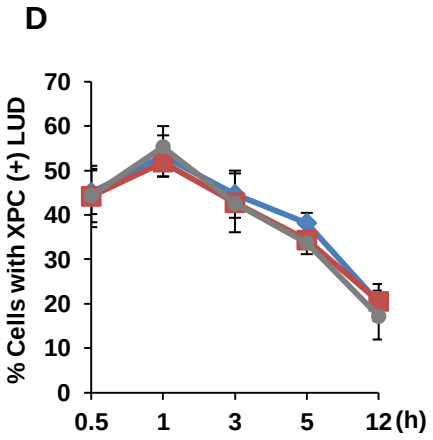

Supplemental 2

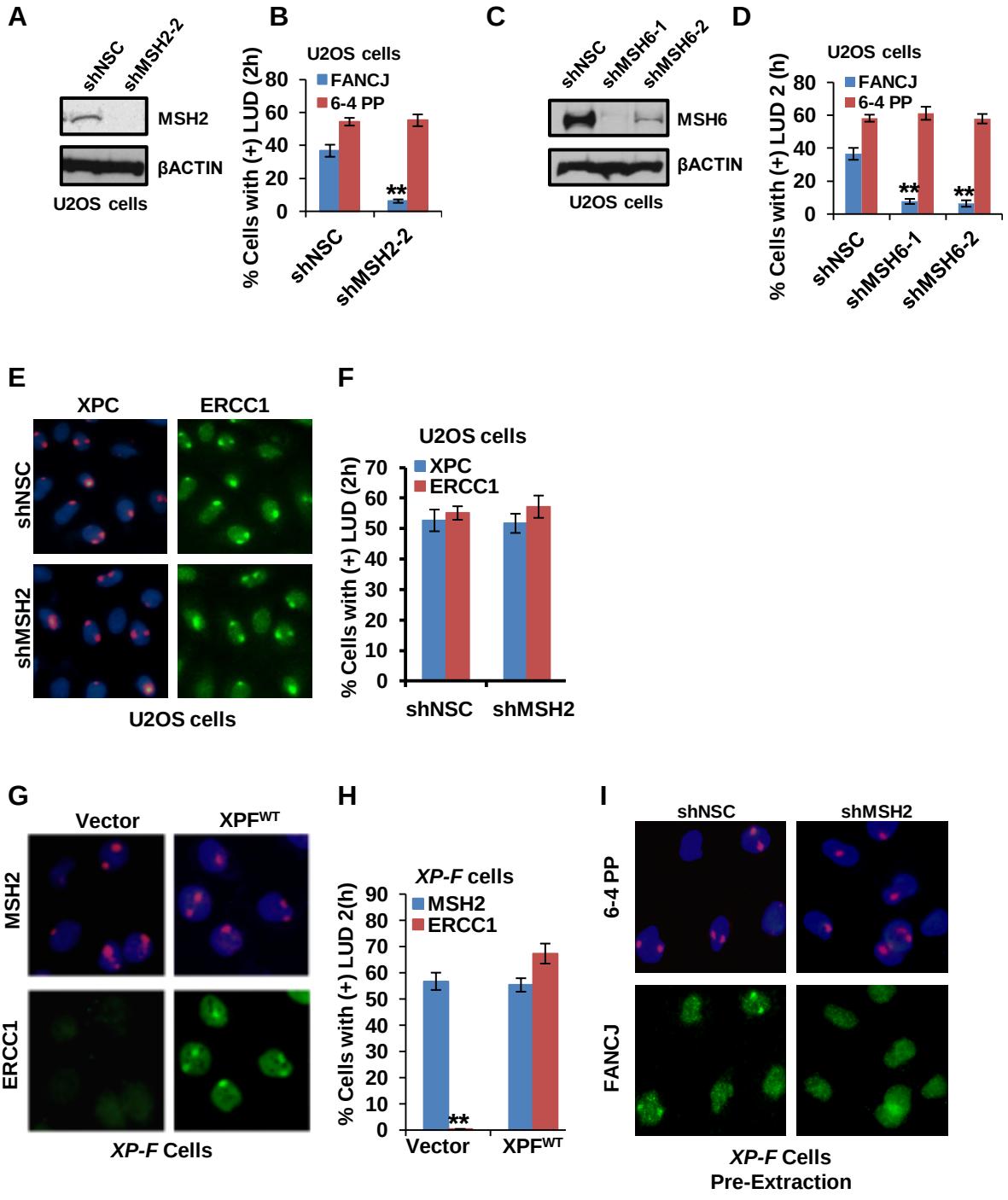

Supplemental 3

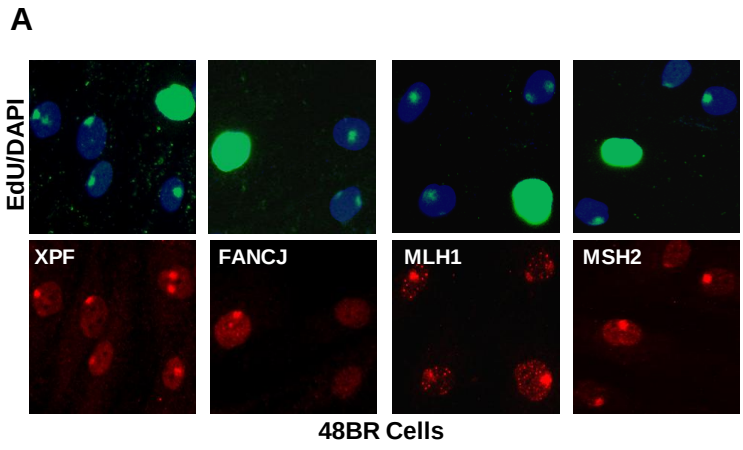

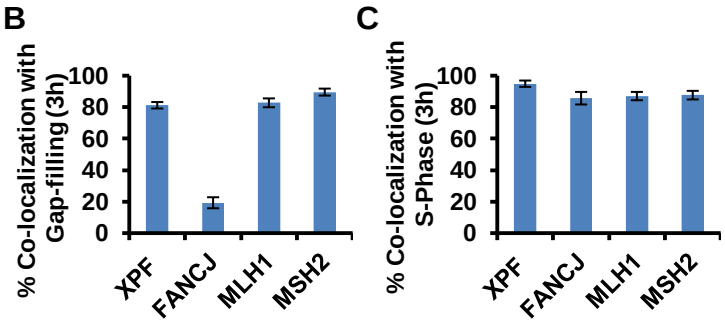

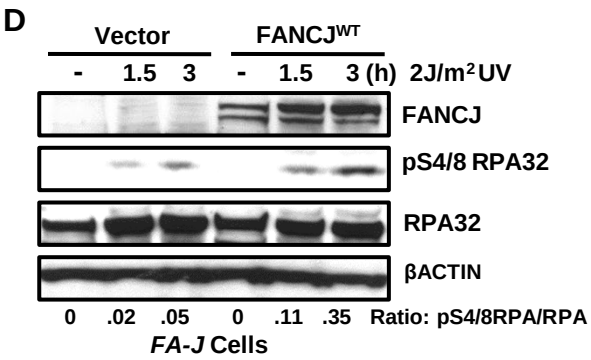

Supplemental 4

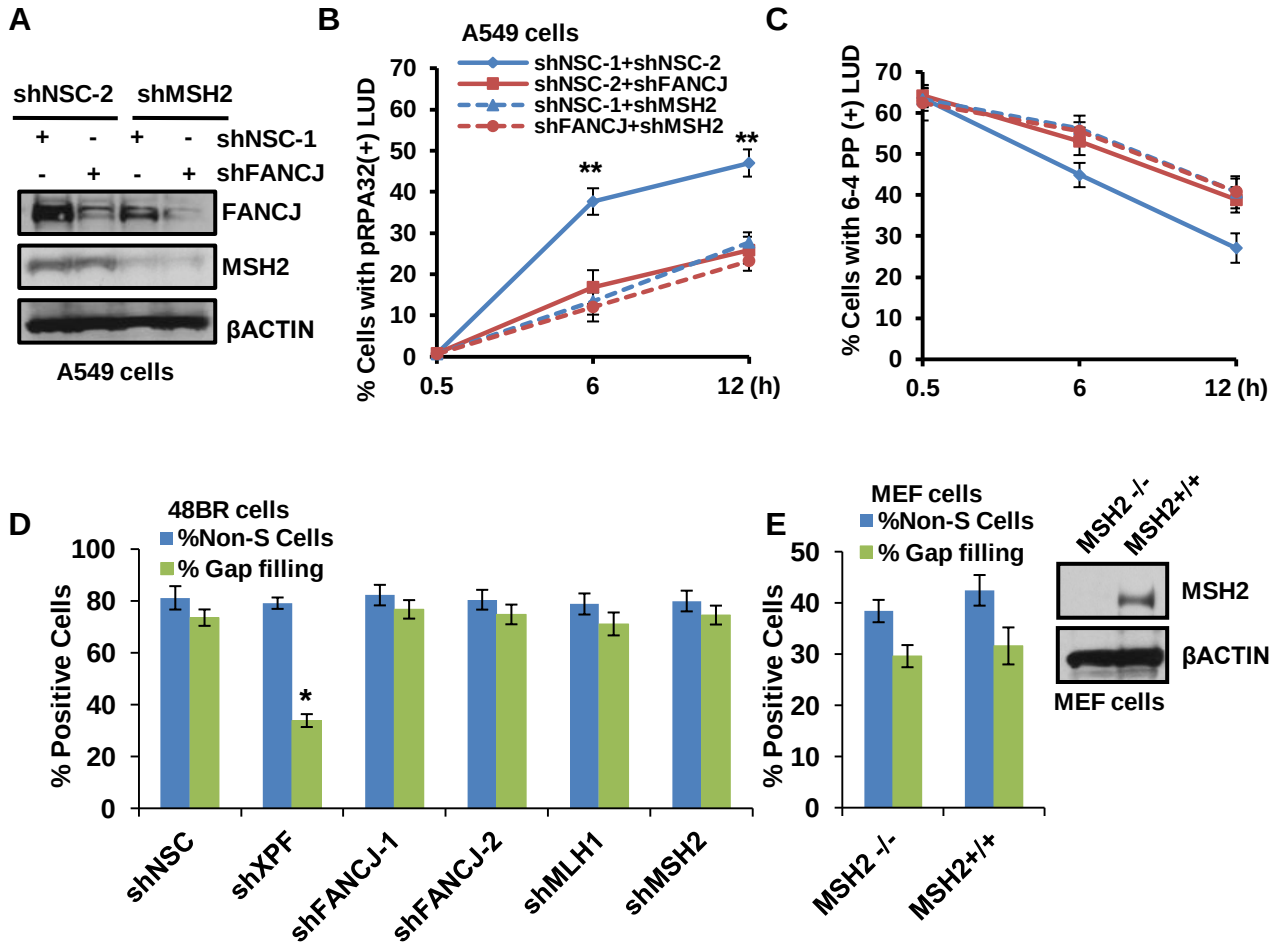

Supplemental 5

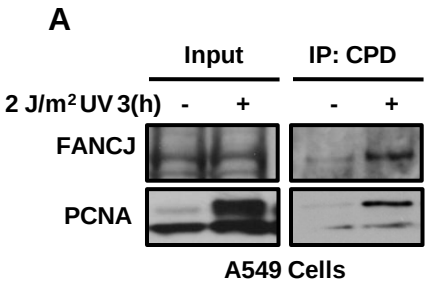

Supplemental 6

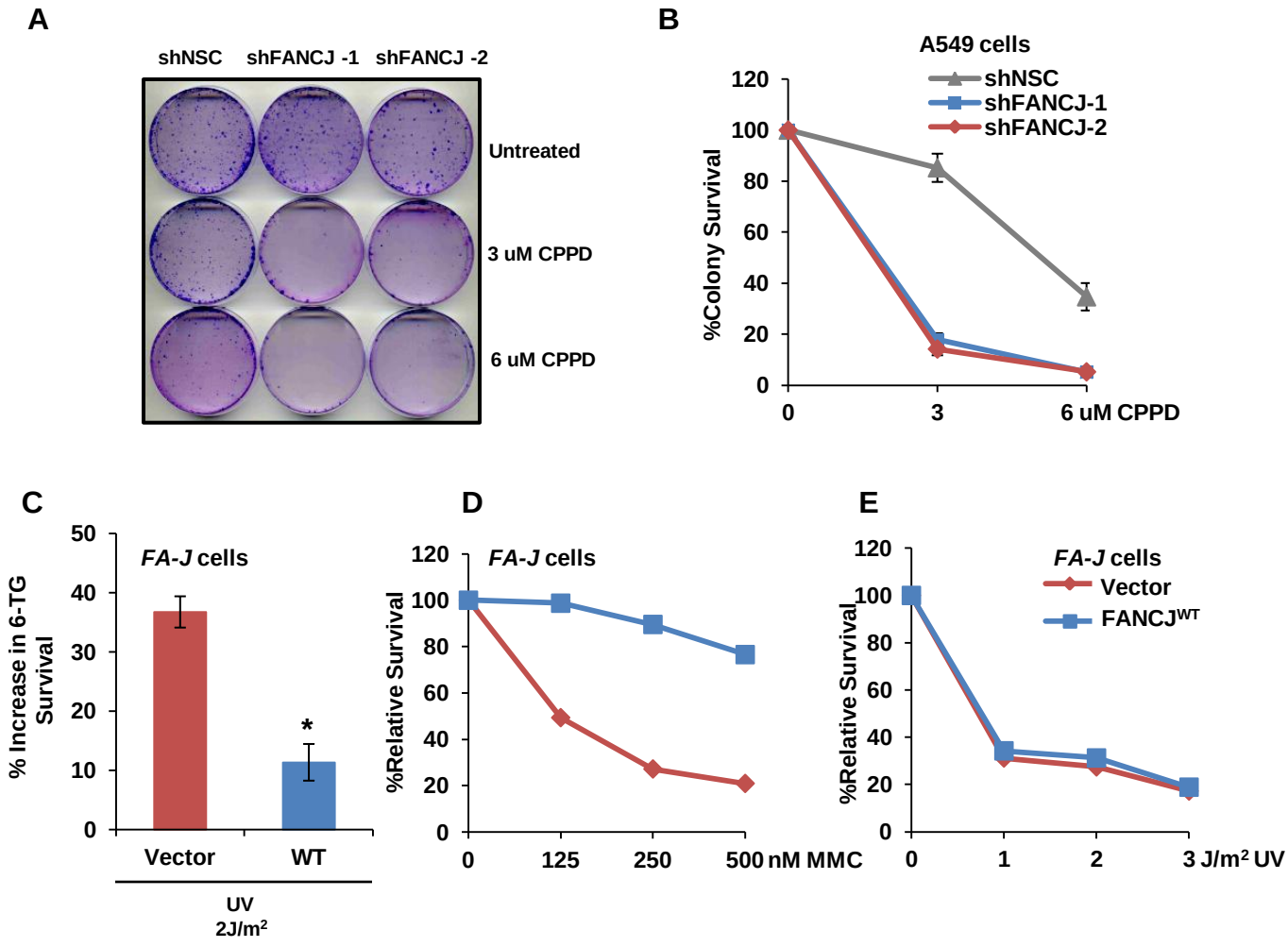

Supplemental 7

A

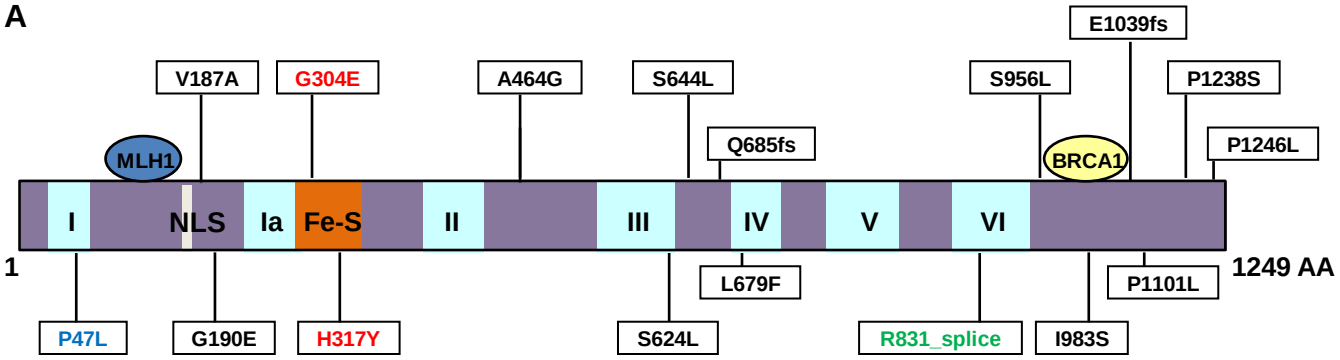

B

FANCJ	Type
P47L	Missense
V187A	Missense
G190E	Missense
G304E	Missense
H317Y	Missense
A464G	Missense
S624L	Missense
S644L	Missense
L679F	Missense
Q685*	Nonsense
R831_splice	Splice Site
I983S	Missense
S956L	Missense
E1039fs	Frameshift
P1101L	Missense
P1238S	Missense
P1246L	Missense

C

MSH2	Type
Q395*	Nonsense
P476S	Missense
L478F	Missense (Squamous)
R680*	Nonsense
C822F	Missense

D

MSH6	Type
K155R	Missense
R240*	Nonsense
G306K	Missense
A457V	Missense
P623L	Missense
S677I	Missense
T757I	Missense
M868I	Missense
Q939*	Nonsense
T1008I	Missense
T1219I	Missense

E

MLH1	Type
R217C	Missense
H315Y	Missense
T347I	Missense
S368L	Missense
L507*	Nonsense
L521fs	Frameshift
p.? (c.1732-1G>A)	Intronic

F

PMS2	Type
S769F	Missense
K178R	Missense
S769F	Missense
R151C	Missense
S128L	Missense
H634Y	Missense
H552R	Missense

Supplemental 8

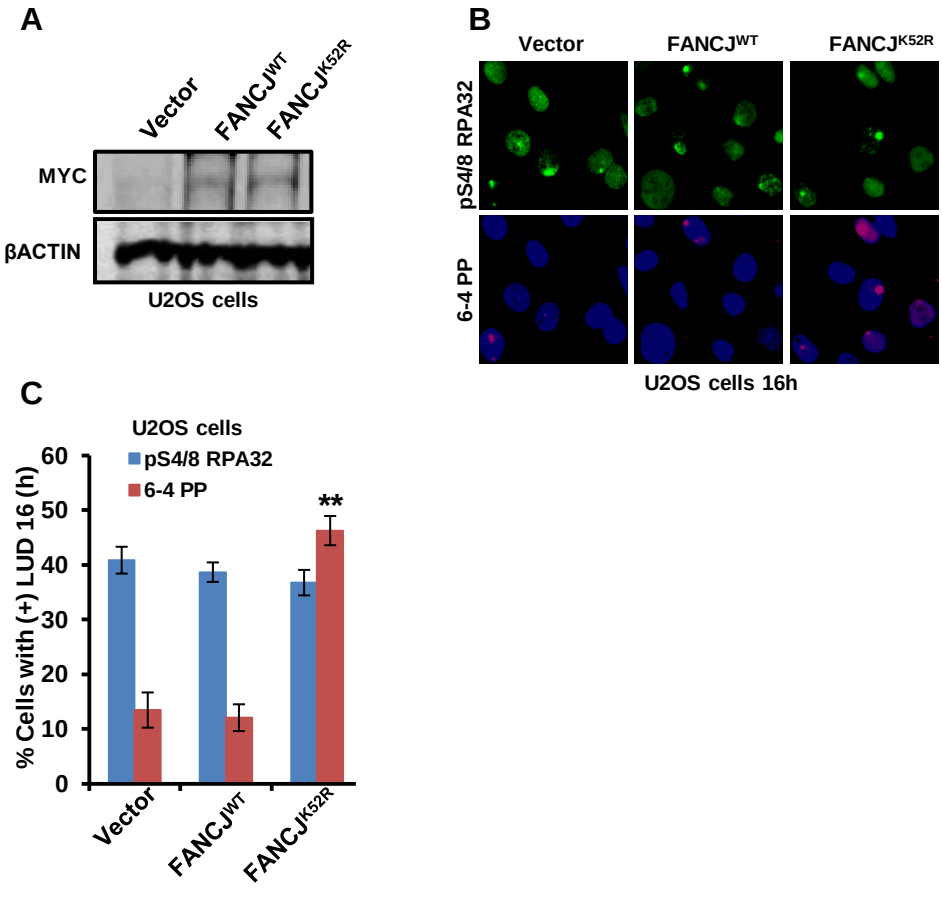

Supplemental 9

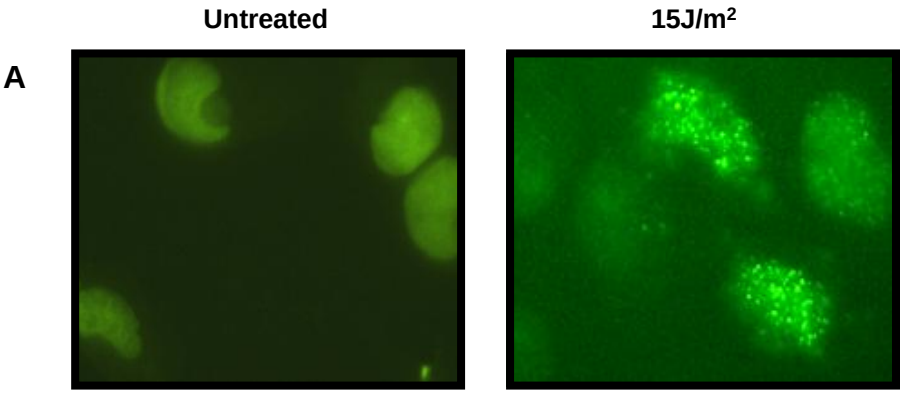

GFP-polh
U2OS cells

B

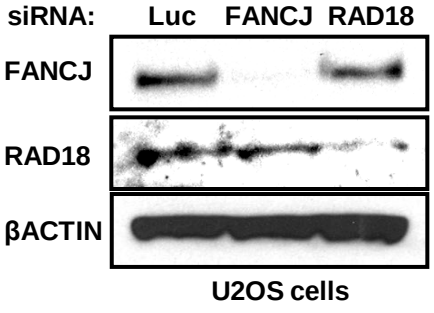

C

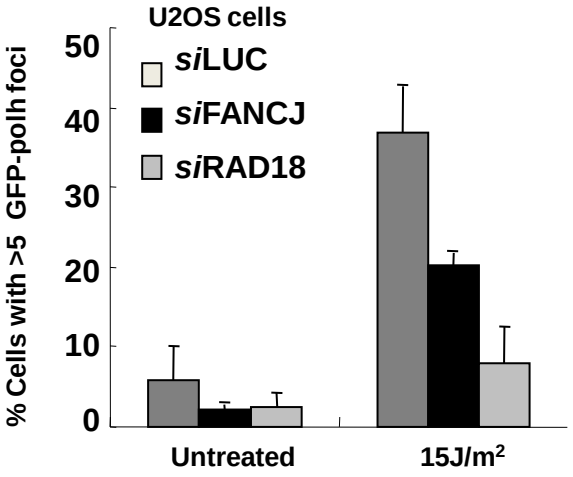

Supplemental Table 1

#Clones	Position (Strand) (NTS+; TS-)	(Sequence Change (5'->3')	Exon	Amino Acid
shNSC				
2	97(-)	CTTT(C>T)CAAA	2	Glu->Lys
1	112(+)	TATT(C>T)CTCA	2	Pro->Ser
1	260(-)	ATTT(C>T)TATT	3	Arg->Lys
3	400(-)	TCTT(C>T)CACA	5	Glu->Lys
1	443(+)	CTTT(C>T)CTTG	6	Ser->Phe
1	374(+)	ACTT(T>C)AACT	4	Leu->Ser
1	297(+)	ATTT(T>A)ATCA	3	Phe->Leu
1	374(+)	ACTT(T>A)AACT	4	Leu->Stop
shFANCJ 1+2				
5	112(+)	TATT(C>T)CTCA	2	Pro->Ser
4	145(+)	ACGT(C>T)TTGC	3	Leu->Phe
1	149(+)	CTTG(C>T)TCGA	3	Ala->Val
3	212(-)	ATAG(C>T)CCCC	3	Gly->Asp
1	227(+)	TTTG(C>T)TGAC	3	Ala->Val
9	260(-)	ATTT(C>T)TATT	3	Arg->Lys
7	272(-)	GGAT(C>T)TATC	3	Arg->Lys
3	275(+)	AGAT(C>T)CATT	3	Ser->Phe
2	280(+)	CATT(C>T)CTAT	3	Pro->Ser
1	281(+)	ATTC(C>T)TATG	3	Pro->Leu
3	364(+)	TGAT(C>T)TCTC	4	Leu->Phe
1	379(-)	TTTC(C>T)AGTT	4	Gly->Arg
2	380(-)	CTTT(C>T)CAGT	4	Gly->Glu
6	400(-)	TCTT(C>T)CACA	5	Glu->Lys
2	412(-)	GTGT(C>T)AATT	6	Asp->Asn
1	443(+)	CTTT(C>T)CTTG	6	Ser->Phe
7	500(-)	GGTC(C>T)TTTT	7	Arg->Lys
3	509(-)	ACTT(C>T)GTGG	7	Arg->Gln
5	544(-)	ATTT(C>T)AAAT	8	Glu->Lys
3	224(+)	TTCT(T>C)TGCT	3	Phe->Ser
2	296(+)	GATT(T>C)TATC	3	Phe->Ser
2	367(+)	TCTC(T>C)CAAC	4	Ser->Pro
3	437(+)	ACTT(T>C)GCTT	6	Leu->Ser
1	532(+)	AGAC(T>C)TTGT	7	Phe->Leu
3	263(-)	ACTA(T>A)TTTC	3	Asn->Ile
1	407(+)	GATA(T>A)AATT	6	Ile->Lys
1	409(-)	TCAA(T>A)TATA	6	Ile->Phe
1	543(+)	GATT(T>A)GAAA	8	Phe->Leu
1	280(+)	CATT(C>G)CTAT	3	Pro->Ala
1	443(+)	CTTT(C>G)CTTG	6	Ser->Cys